International Journal of BioMedicine 4(2) (2014) 109-113

INTERNATIONAL JOURNAL OF BIOMEDICINE

MODERN MEDICAL EQUIPMENT

X-Ray Diffraction Technique in the Analysis of Phases of Hydroxylapatite and Calcium Phosphate in a Human Jaw

Srđan D. Poštić, PhD*

Clinic of Dental Prosthetic,University School of Dental Medicine, University of Belgrade Belgrade, Serbia

Abstract

Objective: Human jawbones consist mainly of hydroxylapatite. The aim of this study was to assess the structure of solid calcium phosphate compounds of the jaw bone (JB) in cases of normal and osteoporotic JBs.

Design: The X-ray diffraction technique was used to analyze the structure of samples of cadavers' jawbones. The experimental JB samples were taken from an osteoporotic and atrophic jawbone, and control samples were from normal and nonosteoporotic bone samples.

Results: Hydroxylapatite was the only phase in control bone samples. In experimental bone samples, the above-mentioned phase was registered, as well as monetite and brushite.

Conclusion: The obtained data indicated that the changes of crystalographic forms of calcium phosphate in the physiologic system were balanced according to the possibility of change in the inorganic chemical system.

Keywords: *X-ray diffraction; mineralized tissues; bone; jaw.*

Introduction

Calcium orthophosphates are important compounds in biological systems because calcium is the main mineral constituent of bones [1,2]. These compounds materialize in various forms (Table 1) [1], but for jawbones, which were investigated in this study, the most important compounds of calcium are hydroxylapatite (HAp) $Ca_{10}(PO_4)_6(OH)_2$ (in some publications [2,5], the formula $Ca_5(PO_4)_3(OH)$ has been cited), monetite (monoclinic or hexagonal) (M) $CaHPO_4$ (monoclinic) and brushite (B) $CaHPO_4{\cdot}2H_2O$ (triclinic) [1]. The existence of amorphous phases [3,4] of calcium phosphate was also registered. The solubility products [1] at 37ºC are $L=9.2\cdot10^{-7}$ for monetite, $L=1.87\cdot10^{-7}$ for brushite, and $L=5.5\cdot10^{-118}$ for hydroxyapatite. However, in another report [5], the value of $L=2.27\cdot10^{-58}$ at 37ºC for hydroxylapatite is different. Brushite is formed by mixing the solutions of $CaCl_2$ (0.01–0.08 mol/l) and $NaHPO_4\cdot H_2O$ (0.005–0.08 mol/l), at pH<7.1, at 25ºC. However, at pH=7.1 and higher, amorphous sediment of calcium phosphate is formed, in which the ratio of Ca:P=1.47. In the mixture of the calcium hydroxide suspension and orthophosphoric acid solution, five consecutive levels of the reaction were identified [6], in which previously formed hydroxylapatite was transformed to brushite with a solubility product in the temperature function [6] of $L=e^{(8403/T+41.8-0.97\,T)}$. At 37ºC and pH=6, the rate of brushite formation is more than 1000 times higher than the rate of formation of hydroxylapatite. In water solution with an initial pH=10.8, at a temperature of 39ºC, after a prolonged period of hydrolysis, brushite is transformed into hydroxylapatite, which is deficient in calcium [7], but after more prolonged hydrolysis, it is transformed into hydroxylapatite. The addition of Ca^{++} ions accelerates the formation of HAp. Therefore, amorphous calcium phosphate has the role in the processes of formation of crystal calcium phosphate [8]. The synthetic hydroxyapatite [9], which is used in production of artificial teeth and artificial jaws, is of a different structure compared to natural hydroxylapatite, mainly because of different crystallinity, which has been changed by mechanical crushing and mixing of particles, and during temperature processing. Thus, many scientific explanations are focused on characterizing the group of chemical compounds, consisting mainly of calcium phosphates, that are used as basic structures in the fabrication of orthopaedic and dental cements [9]. The influence of modality in the fabrication of hydroxylapatite was assessed, as well as the mode of purifying it with a strictly defined relationship of granulations of wet

Corresponding author: *Srđan D. Poštić, PhD. Clinic of Dental Prosthetic, School of Dental Medicine, University of Belgrade.E-mail: srdjan.postic@stomf.bg.ac.rs*

and dry particles, for compression of the final product [10,11]. Certain studies support the selection of $Ca_5(PO_4)_3(OH)$.

Detection of calcium and phosphorus contents in the JB at the location where natural teeth are connected to the bones of osteoporotic people showed decreased levels of minerals in the environments assessed [12].

In the solutions, which simulate body fluid (artificial saliva, artificial serum etc), the precipitation of calcium phosphate was investigated theoretically [13] as well experimentally [14-16] by dissolving these compounds [17-19], and the synthesis of different forms of calcium phosphates and their transformations [20-22] was used to fabricate bioceramics and for various usages of bioceramics.

Table 1.

Calcium Orthophosphate Minerals[1]

Compound	Ca/P molar ratio	Formula	Space group	-logK (37^0)*
Brushite (DCPD)	1.00	$CaHPO_4 \cdot 2\,H_2O$	monoclinic, Ia	6.73
Monetite(DCPA)	1.00	$CaHPO_4$	triclinic P1	6.04
Octacalcium-phosphate (OCP	1.33	$Ca_8(HPO_4)_2(PO_4)_4 \cdot 5\,H_2O$	triclinic P1	98.
Amorphous calcium phosphate (ACP)	1.20-2.20	$Ca_xH_y(PO_4)_z \cdot nH_2O$ N=3-4;5;14-20%H_2O		
α-tricalcium-phosphate (α-TCP)	1.50	$\alpha\text{-}Ca_3(PO_4)_2$	monoclinic $P2_1/a$	28.5
B-tricalcium-phosphate (β-TCP)	1.50	$\beta\text{-}Ca_3(PO_4)_2$	rombohedral R3Ch	29.6
Hydroxylapatite (HAP)	1.67	$Ca_{10}(PO_4)_6(OH)_2$	monoclinic $P2_1/b$, or hexagonal $P6_3/m$	117
Fluoroapatite (FAP)	1.67	$Ca_{10}(PO_4)_6F_2$	hexagonal $P6_3/m$	122.3

**K-Solubility product*

Bone consists of different solid chemical compounds. The content as well as the structure of the solid phase should influence macro-appearance and bone strength. However, some solid compounds in bone could be gradually transformed to other compounds. So far, there are not many reports in the literature about these assumptions [23-25]. Stoichiometric hydroxylapatite (CaO/P_2O_5), hydroxylapatite (HAp), monetite, and brushite compounds have been reported in the literature, as the specific forms present in the bone's solid phase [1-4,8, 11-12].

The aim of this study was to assess the structure of solid calcium phosphate compounds of the jawbone in cases of normal and osteoporotic JBs.

Material and Methods

Samples

Bone samples were carefully extracted from the lower jawbones of cadavers. Written consent and approval for using cadaveric materials was obtained from the responsible medical institution, the Institute for Forensic Medicine in Belgrade.

The samples were similar in dimensions. Two types of bone samples were provided: 1) experimental samples (E) with changed atrophic and osteoporotic structures and 2) control samples (C) taken from the normal bone. The existence of osteoporosis was proposed. Two sample's probes of each sort were used (E_1 and E_2, C_1 and C_2). Samples E_1 and C_1 were obtained from complete bone samples, but samples E_2 and C_2 were obtained from the exterior layer of the corresponding bone. Samples were isolated, cleaned, and degreased in acetone with the intention of preparing them for examination [13,14,26]. After drying and storage in vacuum conditions, samples were mechanically dusted in agate mortar.

X-ray diffraction analysis

X-ray diffraction analysis was applied to detect the phases and compounds of samples of jawbones. A powder mixture was placed in a diffractometer (Crystalloflex diffractometer D-500, Siemens). An electrical voltage of 35kV with 20 mA was used for this experiment.

Results

In Figures 1 and 2, X-ray diffractograms of E_1 and E_2 samples are presented. The diffractogram of sample C_1 is shown in Figure 1. It is the same as the diffractogram of sample C_2.

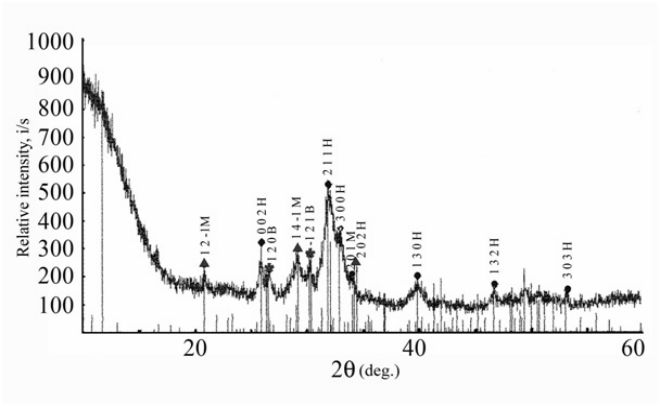

Fig. 1.

Diffractogram of the experimental jow bone sample E_1. H-hydroxylapatite: $Ca_{10}(PO_4)_6(OH)_2$; M-monetite:$CaHPO_4$; B-brushite:$CaHPO_4 \cdot 2H_2O$

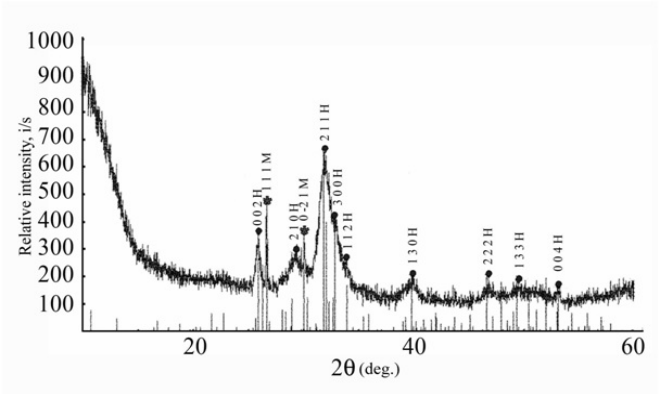

Fig. 2.

Diffractogram of the experimental jow bone sample E_2. H-hydroxylapatite: $Ca_{10}(PO_4)_6(OH)_2$; M-monetite:$CaHPO_4$;

In Table 2, the band positions (2θ, degree) in the diffractograms of samples and relative intensities (i/s) are given. In Figures 1–3 are given the Miller indexes and

corresponding crystal forms using data from JCPDS-ICDD [29] 72-0713 for brushite, 09-0077 for brushite, syn, 75-1520 for monetite, 70-1425 for monetite, (synthesized), 74-0566 for hydroxylapatite, 76-0694 for hydroxyapatite, syn, and data from JCPDS [29] (01-074-0565 for hydroxyapatite, 01-072-0713 for brushite, 01-070-0359 for monetite, syn).

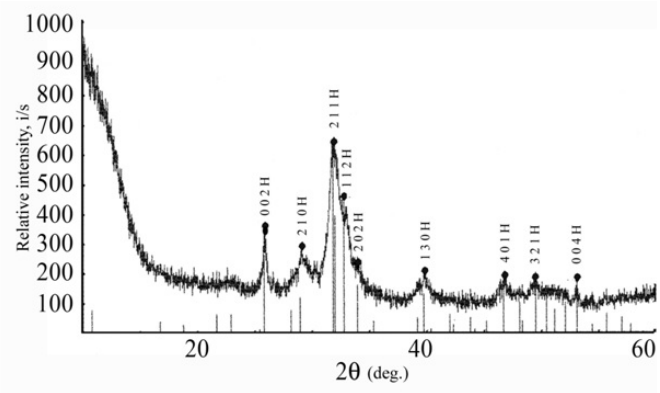

Fig. 3.
Diffractogram of the control jaw bone sample C_1. H-hydroxyapatite: $Ca_{10}(PO_4)_6(OH)_2$

In all samples hydroxylapatite (bands marked H) is present. In the sample E_1 monetite (M) and brushite (B) are present simultaneously with hydroxylapatite. In the sample E_2 monetite is present too. The hydroxylapatite $Ca_{10}(PO_4)_6(OH)_2$ was the dominant phase in samples C_1 and C_2, since bands of other kinds are not present, or their concentration is less than the detection limit.

Discussion

Certain comprehensive studies have shown that natural HAp is non-stoichiometric (exhibits a Ca/P ratio higher than 1.67) nanostructured crystals with carbonate groups and traces of different ions such as HPO_2^{-4} Na^+, Mg^{2+}, Sr^{2+}, K+, Cl^- and F^- built into its structure [30,31], a finding that was not completely confirmed in the analysis in the present study. Additionally, the general formula of HAp is $Ca_{14}Ca_{26}(PO_4)_6(OH)_2$, where Ca1 and Ca2 are two different crystallographic positions for 10 calcium atoms. Four calcium atoms are situated in the Ca1 position, and they are surrounded by nine oxygen atoms, which belong to the PO_4 tetrahedra. Six other calcium atoms, which are coordinated by the six O atoms of the PO_4 tetrahedra and by one of the OH^- ions, are placed in the Ca2 site [32-37]. This statement could be also discussed with the results of the present study in which hydroxylapatite was basically assigned as the $Ca_{10}(PO_4)_6(OH)_2$ structure. According to the literature data, the bone mineral apatite is generally considered to be the B-type and mixed AB-type [37-39] with an increase of A-type substituted for apatite in the old bone; hence, B-type HAp is the most abundant apatite in bones of young humans [40].

Data obtained in this study are in agreement with knowledge that osteoporosis is the process of formation of some other crystal forms of calcium phosphate, at least one, monetite, from HAp.

Carbonate is the most abundant substitution in bone mineral with 2.3–8 wt.%, and it has been shown to vary depending on the age of the individual [40,41]. This was confirmed in this study as well.

Consequently, hydroxylapatite replaced by brushite or monetite reduces bone density and hardness, since the density and hardness of monetite (2.93 g/cm^3; 3 Mohs) [42] and brushite (2.32 g/cm^3; $2^1/_2$ Mohs) [43] are less than that of hydroxylapatite (3.16 g/cm^3; 5 Mohs) [44].

Table 3 provides some characteristics of hydroxyapatite in the bone, which is the dominant phase in samples 1–3 (minimal dislocation density (A), microstrain (B) and crystallite radius (D)), calculated from data presented in Table 2, according to the literature [45,46]. The changes of cited values are highest in sample 1, i.e., in the sample with two phases formed through osteoporotic processes.

The change of the crystallographic structure, formation from monetite and brushite by the recrystallization of the hydroxylapatite, also changes the relationship of Ca:P, according to data in Table 1, i.e., the amount of Ca in the osteoporotic bone must be less than in the normal bone. On the basis of these data, it is concluded that the reduction of calcium content in the solution, or physiologic environment, could influence transitions of hydroxylapatite to monetite or to brushite. Also, the formation of Ca^{++} stable complexes with other inorganic or organic compounds due to the change of physiological media can also be the cause of the transformation of the hydroxylapatite into the cited crystal forms.

Table 2.

The 2θ value of the diffraction peaks (deg), relative intensity (i/s), d- spacing (A), (Miller index (h k l) and phase F (H-hydroxylapatite, B-brushite, M-monetite) for samples 1, 2 and 3.

Sample 1					Sample 2					Sample 3				
2θ	i/s	D	h k l	F	2θ	i/s	D	h k l	F	2θ	i/s	D	h k l	F
21.00	250	4.230	1 2 -1	M	25.00	350	3.565	0 0 2	H	26.00	350	3.422	0 0 2	H
26.00	250	3.420	0 0 2	H	25.70	460	3.468	1 1 1	M	29.00	300	3.080	2 1 0	H
27.00	220	3.304	1 2 0	B	28.00	300	3.182	2 1 0	H	30.50	650	2.928	2 1 1	H
29.00	300	3.080	1 4 -1	M	28.70	370	3.100	0 -2 1	M	32.50	450	2.750	1 1 2	H
30.00	300	2.664	-1 2 1	B	31.00	680	2.884	2 1 1	H	34.00	220	2.637	2 0 2	H
31.00	550	2.884	2 1 1	H	32.00	410	2.790	3 0 0	H	40.00	200	2.251	1 3 0	H
33.00	400	2.711	3 0 0	H	33.00	300	2.711	1 1 2	H	46.00	200	1.969	4 0 1	H
34.00	250	2.750	2 0 1	M	39.00	200	2.305	1 3 0	H	50.50	190	1.808	3 2 1	H
34.50	200	2.637	2 0 2	H	46.50	200	1.949	2 2 2	H	53.00	185	1.726	0 0 4	H
40.00	200	2.251	1 3 0	H	49.00	190	1.892	1 3 3	H					
48.00	180	1.892	1 3 2	H	54.00	180	1.696	0 0 4	H					
53.00	150	1.737	3 0 3	H										

Table 3.

Characteristic values of the hydroxylapatite crystal in the investigated bone samples calculated using data from the Table 2.

Sample	2θ*	Phase	$Dx10^{-10}$ m	Am^{-2}	B %
1	32.06	Hydroxyapatite	89.15	3.77×10^{16}	0.802
2	31.25	Hydroxyapatite	62.5	7.68×10^{16}	1.178
3	29.90	Hydroxyapatite	62.3	7.73×10^{16}	1.269

The results of this work provide a particular set of data that specify characteristic diffraction peaks and phases in experimental atrophic and osteoporotic bones of cadavers in contrast to data obtained for regular structure of the control JBs of separate cadavers.

Conclusion

On the basis of X-ray analysis, forms of calcium phosphate, monetite and brushite, as well as hydroxylapatite, were established in osteoporotic samples, whereas only the hydroxylapatite compound was present in the normal bone sample. This result is the consequence of the basic chemical characteristics of the samples.

References

1. Wang L, Nancollas GH. Calcium orthophosphates: Crystallization and Dissolution. Chem Rev 2008; 108(11):4628-69.
2. Arifuzzaman SM, Rohani S. Experimental study of brushite precipitation. J Crystal Growth 2004; 267(3-4):624-34.
3. Christoffersen J, Christoffersen MR, Kibalczyc W, Andersen FA. A contribution to the understanding of the formation of calcium phosphates. J Crystal Growth 1989; 94(3):767-77.
4. Boistelle R, Lopez-Valero I. Growth units and nucleation: The case of calcium phosphates. J Crystal Growth 1990; 102(3):609-17.
5. Chen ZF, Darvell BW, Leung VWH. Hydroxyapatite solubility in simple inorganic solutions. Arch Oral Biol 2004; 49(5):359-67.
6. Oliviera C, Ferreira A, Rocha F. Dicalcium Phosphate Dihydrate Precipitation: Characterization and Crystal Growth. Chemical Engineering Research and Design 2007; 85(12):1655-61.
7. Štulajterová, R., Medvecký, L. Effect of calcium ions on transformation brushite to hydroxyapatite in aqueous solutions. Colloids and Surfaces A: Physicochem Eng Aspects 2008; 316(1-3):104-9.
8. Tenhuisen KS, Brown PW. The kinetics of calcium deficient and stoichiometric hydroxyapatite formation from CaHPO4·2H2O and Ca4(PO4)2O. J Mat Science Mater Med 1996; 7(6):309-16.
9. Nakano T, Umakoshi Y, Tokumura A. Variation in crystallinity of hydroxyapatite and the related calcium phosphates by mechanical grinding and subsequent heat treatment. Metalurgical and Materials Transactions A 2002; 33A(3):521-28.
10. Jalota S, Tas AC, Bhaduri SB. Synthesis of HA-seeded TTCP (Ca4(PO4)2O) powders at 1230°C from Ca(CH3COO)2·H2O and NH4H2PO4. J Amer Ceram Soc 2005; 88(12):3353-60.
11. Pontier C, Viana M, Champion E, Bernache-Assollant D, Chulia D. About the use of stoichiometric hydroxyapatite in compression - incidence of manufacturing process on compressibility. Eur J Pharm and Biopharm 2001; 51(3):249-57.
12. Poštić SD, Marković V, Veselinović D, Mirjanić M, Zec S. Physical-chemic characterisation of osteoporotic bone. J Dent Res 2002; 81(2 Suppl): B284.
13. Lu X and Leng Y. Theoretical analysis of calcium phosphate precipitation in simulated body fluid. Biomaterials 2005; 26(10):1097-108.
14. Bayraktar D, Tas AC. Chemical preparation of carbonated calcium hydroxyapatite powders at 37°C in urea-containing synthetic body fluids. J Europ Ceram Soc 1999; 19(13-14):2573-79.
15. Dorozhkin SV. Bioceramics of calcium orthophosphates. Biomaterials 2010; 31(7):1465-85.
16. LeGeros RZ. Calcium phosphate-based osteoinductive materials. Chem Rev 2008; 108(11):4742-53.
17. Priya A, Nath S, Biswas K, Basu B. In vitro dissolution of calcium phosphate-mullite composite in simulated body fluid. J Mater Sci Mater Med 2010; 21(6):1817-28.
18. Rezvannia MF, Moztarzadeh F, Tahriri M. Formation of hydroxyapatite nanoneedles on the surface of a novel calcium phosphate/blood plasma proteins biocement in simulated body fluid (SBF). J Ceram Process Res 2009; 10(5):669-73.
19. Seo DS, Song DS, Lee JK. Dissolution of calcium phosphate powders with different compositions in simulated body fluid. Key Engineering Materials 2007;342-343:653-656.
20. Kolos EC, Ruys AJ, Rohanizadeh R, Muir M, Roger G. Calcium phosphate fibres synthesized from a simulated body fluid. J Mater Sci Mater Med 2006; 17(11): 1179-89.
21. Liu Y, Shelton RM, Barralet JE. Homogeneous octacalcium phosphate precipitation: Effect of temperature and pH. Key Engineering Materials 2004; 254-256:79-82.
22. Weiner S, Wagner HD. The material bone: structure-mechanical function relations. Annu Rev Mater Sci 1998; 28(1):271–98.
23. Boyde A, Kingsmill VJ. Age changes in bone. Gerodontology 1998; 15(1):25-34.
24. Poštić SD. Analysis of osteoporotic changes in mandible and its clinical significance [PhD thesis]. Belgrade, Serbia: The Faculty of Stomatology, University of Belgrade; 1998: 88-110.
25. Boyde A, Jones SJ. Scanning electron microscopy of bone: Instrument, specimen, and issues. Microsc Res Tech 1996; 33(2):92-120.
26. Zhao G. Interaction of surface energy and microarchitecture in determining cell and tissue response to biomaterials [PhD thesis]. Atlanta, Georgia: Georgia Institute of Technology, 2007. Available at: http://smartech.gatech.edu/handle/1853/24656 (accessed September 15, 2010).
27. http: //www.science.smith.edu /departments/ SEM / Manual 99.pdf Internet 2014 [cited 19. Januar 2013].
28. Smith DK and Jenkins R. The powder diffraction file: Past, present, and future. J Res Nath In Technol 1996; 101(3):259-71.
29. The International Centre for Diffraction Data (ICDD) [Internet] 2014 cited February 14, 2011]. Available from: http://www.icdd.com/index.htm.
30. Figueiredo M, Fernando A, Martins G, Freitas J, Judas F, Figueiredo H. Effect of the calcination temperature on the composition and microstructure of hydroxyapatite derived

from human and animal bone. Ceram Inter 2010; 36(8):2383–93.
31. Yao F, LeGeros J, LeGeros RZ. Simultaneous incorporation of carbonate and fluoride in synthetic apatites: Effect on crystallographic and physico-chemical properties. Acta Biomater2009; 5(6):2169–77.
32. White TJ and Dong ZL. Structural derivation and crystal chemistry of apatites. Acta Crystallogr B 2003; 59(Pt 1):1–16.
33. Kannan S, Goetz-Neunhoeffer F, Neubauer J, Ferreira JMF. Ionic substitutions in biphasic hydroxyapatite and β-tricalcium phosphate mixtures: Structural analysis by Rietveld refinement. J Am Ceram Soc 2008; 91(1): 1–12.
34. Ma X, Ellis DE. Initial stages of hydration and Zn substitution/occupation on hydroxyapatite (0001) surfaces. Biomaterials 2008; 29(3):257–65.
35. De Leeuw NH. Local ordering of hydroxy groups in hydroxyapatite. Chem Commun (Camb) 2001; 17:1646–47.
36. Badraoui B, Aissa A, Debbabi M. Structure refinements of cadmium substituted lead fluoroapatites by powder x-ray pattern fitting. J Phys Chem Sol 2007; 68(2): 211–16.
37. Rey C, Collins B, Goehl T, Dickson I R, Glimcher MJ. The carbonate environment in bone mineral: a resolution-enhanced Fourier Transform Infrared Spectroscopy Study. Calcif Tissue Int 1989; 45(3):157–64.
38. Xiao J, Zhu Y, Ruan Q, Liu Y, Zeng Y, Xu F, Zhang L. Biomacromolecule and surfactant complex matrix for oriented stack of 2-dimensional carbonated hydroxyapatite nanosheets as alignment in calcified tissues. Cryst Growth Des 2010; 10(4):1492–99.
39. Emerson WH and Fischer ED. The infra-red absorption spectra of carbonate in calcified tissues. Arch Oral Biol 1962; 7(6):671–83.
40. Zhou WY, Wang M, Cheung WL, Guo BC, Jia DM. Synthesis of carbonated hydroxyapatite nanospheres through nanoemulsion. J Mater Sci Mater Med 2008; 19(1):103–10.
41. Gibson IR, Bonfield W. Novel synthesis and characterization of an AB-type carbonate-substituted hydroxyapatite. J Biomed Mater Res 2002; 59(4):697–708.
42. Monetit [Internet] 2014 [cited 19. June 2013]. Available from: http://www.mindat.org/min-2755.html.
43. Brushite [Internet] 2014 [cited 09. Januar 2014]. Available from: http://www.mindat.org/min-793.html.
44. Hydroxylapatite [Internet] 2014 [cited 10 Januar 2014]. Available from: http://www.mindat.org/min-1992.html.
45. Klug HP, Aleksander LE. X-Ray Diffraction Procedures for polycrystalline and amorphous materials. 2nd ed. New York: John, Wiley&Sons; 1974.
46. Williamson GK, Smallman RE. III. Dislocation densities in some annealed and cold-worked metals from measurements on the X-ray debye-scherrer spectrum. Philosophical Magazine 1956; 1(1):34-36.